Improving the comb drive actuator transient response using Digital Compensation Technique

M. S. Mahmoud[(1)] , D. Khalil[(2,3)] , M. T. El-Hagry[(1)] and M. A. Badr[(2)]

(1) Electronics Research Institute: National Research Center, El-Tahrer St. Dokki, Cairo12622 , Egypt.

mostafa_mahmoud74@yahoo.com

(2) Ain Shams University, faculty of engineering, 1 El-srayat St., Abbsia, Cairo, Egypt.

(3) MEMScAP Egypt: 9, Ibn Battouta St. Heliopolis, Cairo11341, Egypt Fax: (+202) 4146492.

diaa.khalil@memscap.com

ABSTRACT

In this work we propose a new technique to improve the transient response of the comb drive actuator using a digital compensation technique. This technique is mainly based on the use of a specific digital pulse train that satisfies the equal area criterion on the force displacement diagram of the actuator. Applying this technique to a specific actuator design, we show that it enables to increase the forward displacement without sticking, reduce the overshoot, and improve the speed of response.

INTRODUCTION

Linear comb drive actuators (CDA) are very important MEMS structures that are widely used in many applications [1,2]. They are currently used in force-balanced accelerometers, resonant accelerometers, opto-mechanical subsystems and others [4-7]. Current CDA step response is characterized by limited forward displacements and strong overshoot [8]. Many techniques have been proposed to improve the step response to minimize the overshoot and/or the settling time of the actuator by adding extra network controllers or series resistances as electrically damping elements or by optimizing the comb finger structure [9-10]. The basic idea in the digital compensation depends on the fact that, the overshoot in the comb drive response is mainly due to the excess energy stored in the actuator during its acceleration by the applied voltage. In our technique, the energy supplied to the CDA is just enough to enable the shuttle to reach the designed destination.

COMB DRIVE ANALYSIS

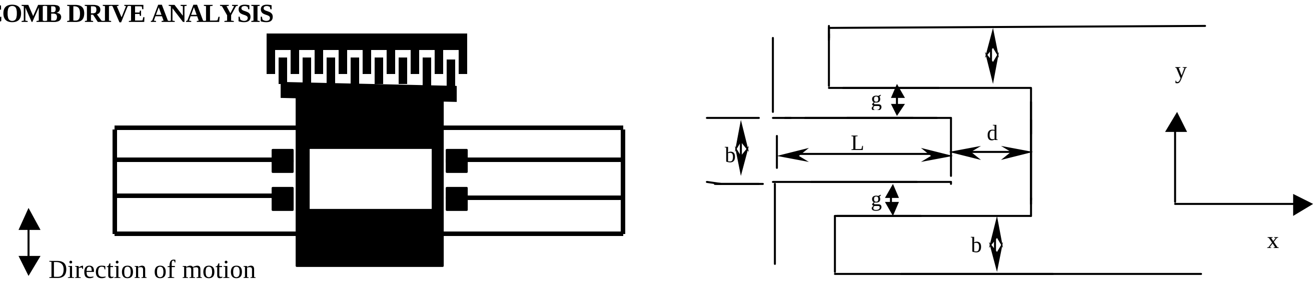

Fig.1. a- Schematic representation of the CDA. , b- Geometrical details of the drive fingers.

A schematic representation of the analyzed CDA is shown in Fig. 1-a with geometrical details of on of its fingers in Fig. 1-b. When a potential deference V is applied between moving and fixed fingers an electrostatic driving force F_e is generated and the shuttle is displaced in the x-direction [6,9] against a restoring spring force F_s .

$$Fe = Fp+F_f\text{, where, } F_f= 1.12n\varepsilon tV^2/g\ ,\ F_p = n\varepsilon tbV^2/(d-x)^2 \qquad (1)$$

Where n is the number of moving fingers and ε is the dielectric constant of air and the other geometrical parameters are defined in Fig. 1-b. It is clear that F_p is the main reason of the front sticking.

The dynamic response of the CDA could be expressed by the simple equation of motion (2), where m_{eff} is the effective mass, b_f is the damping coefficient and k is the restoring spring force, F_p can be ignored in calculating the response.

In this case the CDA is simply a second order system, whose response to a step voltage is exponentially damped sinusoidal wave.

$$m_{eff}\frac{\partial^2 x(t)}{\partial t^2}+b_f\frac{\partial x(t)}{\partial t}+kx(t)=F_e\cong F_f \qquad (2)$$

Stability equal area criterion

Considering the Force-Displacement diagram of Fig. 2 we have two intersection points B and G at two different displacements x_1 (stable position) and x_3 (unstable position). The dynamic behavior of the CDA can be thus described, from the energy point of view, as follows:

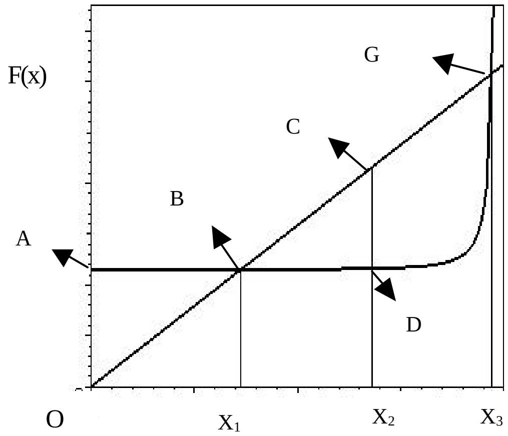

Fig. 2. Force-Displacement diagram of CDA.

At $0 \le x \le x_1$: $F_e > F_s$, so the shuttle will move in the x-direction until it reaches position x_1. At this point, the electrical energy (E_{elec}) is given by area {OABX$_1$0}, some of this energy is stored in the spring (E_{spr}) Area {OBXO}) and the rest (assuming no dissipation) is gained by the shuttle as an accelerating energy (E_{acc}) given by area {OABO}.
At $x=x_1$: $F_e = F_s$, the accelerating energy is still stored in the shuttle and the shuttle will overshoot to a more advanced position x_2 (see Fig.(2)) at which its velocity is zero.
For $x_1 \le x \le x_2$: In this region, $F_e < F_s$ and thus the net force is a retarding force and a decelerating energy (E_{decc})is developed. This energy is given by area (BCDB).
At $x=x_2$ (first overshoot) and the stored (gained) energy ($E_{acc.}$) is completely stored in the spring. However, $x=x_2$ is not an equilibrium position and the shuttle moves back again in the negative x-direction and oscillates around the steady state position x_1 until this oscillating energy is completely dissipated in the friction and the shuttle settles at x= x_1.
So, the criterion for stability requires that $x_2<x_3$, i.e. the area OAB0 must not be greater than the sum of areas (BCGDB) plus the energy dissipated in friction (E_{fr}) during shuttle motion to reach the fit overshoot in time t_{peak} (peak time).

$$E_{fr} = \int_0^{t_{peak}} b_f \left(\frac{\partial x}{\partial t}\right)^2 dt \qquad (3)$$

Using this technique, the maximum (critical) applied step voltage (V_{max}) that can be applied without sticking and maximum steady state position x_1 could be calculated, at x_2, the total system energy is equal to zero. Thus, the maximum allowable overshoot (without sticking) takes place when x_2=x_3 and the spring force is equal to the total electrostatic force, i.e. when:

$$\mathrm{U} = 1.12\frac{net}{g}V^2 x_3 + \frac{netb}{d - x_3}V^2 - \frac{1}{2}k(x_3)^2 - \int_0^{t_{peak}} b_f \left(\frac{\partial x(t)}{\partial t}\right)^2 dt = 0 \qquad (4)$$

and

$$kx_3 = 1.12 * \frac{net}{g}V^2 + \frac{netb}{(d - x_3)^2}V^2 \qquad (5)$$

Solving equations (4) and (5), we get the maximum displacement x_3 under dynamic operation of the actuator as well as the corresponding voltage.

Digital Compensation Technique

The main idea in the digital compensation technique could be illustrated in Fig. 3. If it is required to drive the actuator at a designed position $x_{req.}$ a step voltage is applied for a period of T_1, and the shuttle gains momentum enough displace it to $x_{req.}$ at t = T_2 . To hold the shuttle at that position $x_{req.}$ the voltage is to be applied again at t = T_2 . Similarly, to restore its zero position (V is switched OFF), the overshoot may take place and to avoid it a step voltage pulse (a braking pulse) is applied during the period $T_3<t<T_4$ as shown in Fig. 3. This could be explained by the equal area criterion of stability where, during $0 \le t \le T_1$ the shuttle gains accelerating energy and during $T_1 \le t \le T_2$ it stores the gained energy in the spring. Also some of the accelerating energy is dissipated in the friction and at point D (x=x_2) the total system energy is equal to zero and the applied voltage at that instant is only to an electrostatic force to hold the mass at this position Fig. 3.Now to determine T_1 and T_2 we can easily show that they should satisfy the two conditions:

$\partial x_2(t)/\partial t|_{t=T1} = 0$ (6) and $x_{req.} = x_2(T_2)$ (7)

where x_{req} is the required displacement and $x_2(t)$ is the solution of the actuator equation of motion using the superposition theory [11] and neglecting the small contribution of the non-linear electrostatic force which gives $x_2(t)$ in the form:

$$x_2(t) = \frac{1.12 * \frac{net}{g} V^2}{k} \{ \frac{e^{-xw_n(t-T_1)}}{\sqrt{1-x^2}} \sin(w_d(t-T_1) + \tan^{-1}\frac{\sqrt{1-x^2}}{x}) - \frac{e^{-xw_n t}}{\sqrt{1-x^2}} \sin(w_d t + \tan^{-1}\frac{\sqrt{1-x^2}}{x}) \} \quad (8)$$

Solving equations (6) and (7) we can get T_1 and T_2 for each required displacement. It is to be noted here that both of T_1 and T_2 are dependent on the applied voltage and thus for a given required displacement infinite number of solutions depending on the applied voltage. Similarly, T_3 and T_4 can be obtained by solving:

$x_2(t)|_{t=T4} = 0$ (9) and $\partial x_2(t)/\partial t|_{t=T4} = 0$ (10)

where $x_2'(t)$ is the actuator displacement during $T_3 \leq t \leq T_4$ tacking into account the different initial conditions.
Note, due to the non-linear nature of the electrostatic force Fe, the period (T_4-T_3) is not equal to the period (T_2-T_1).

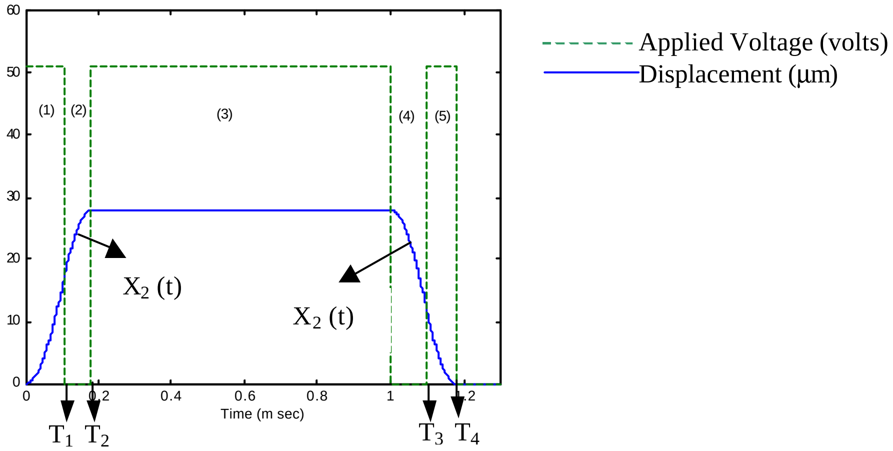

Fig. (3) Overall response of the comb-drive actuator at the different operating regions.

This technique can derive the CDA by a sustained large displacement without sticking Fig. 4. Or periodically at frequencies higher than resonance frequency (eliminating region (3) in Fig. 3) Fig. 5. In our example, t = g = b = 2 µm ,d = 35 µm ,n = 32 fingers ,k = 31.736mN/mt ,b_f = 0.416*10^{-6} Kg/sec^2 ,m_{eff} = 225*10^{-12} Kg, $f_{resonance}$ =1/2π*$(k/m_{eff})^{1/2}$ = 1.89 khz.

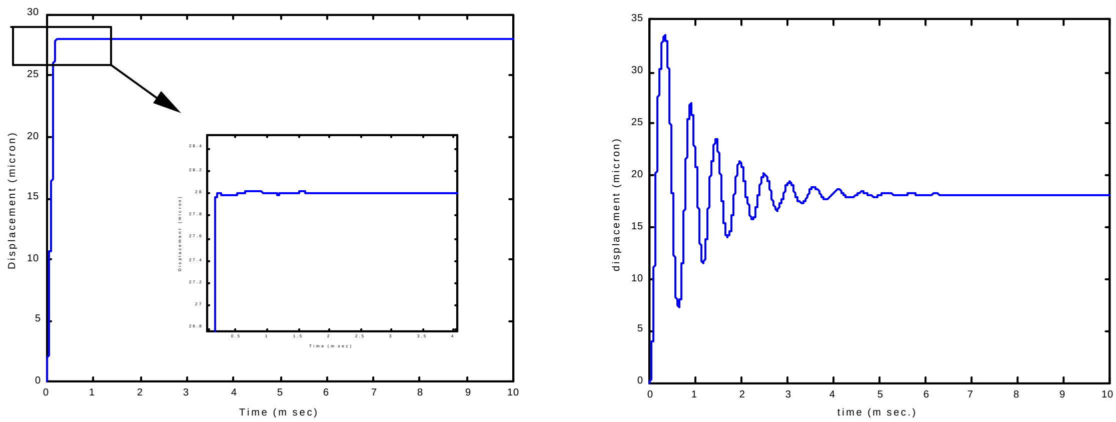

a b

Fig. (4) Response of the comb drive actuator to:

a- A compensated response with V=51.1 volts, x_1 = 28µm,T_1=108.3µsec, T_2=181.3µsec.

b- A step response with V_{max}=41.79 volts, this is max. voltage can applied without sticking without using our technique.

We note also that increasing the applied voltage could increase both the maximum displacement and the operating frequency.

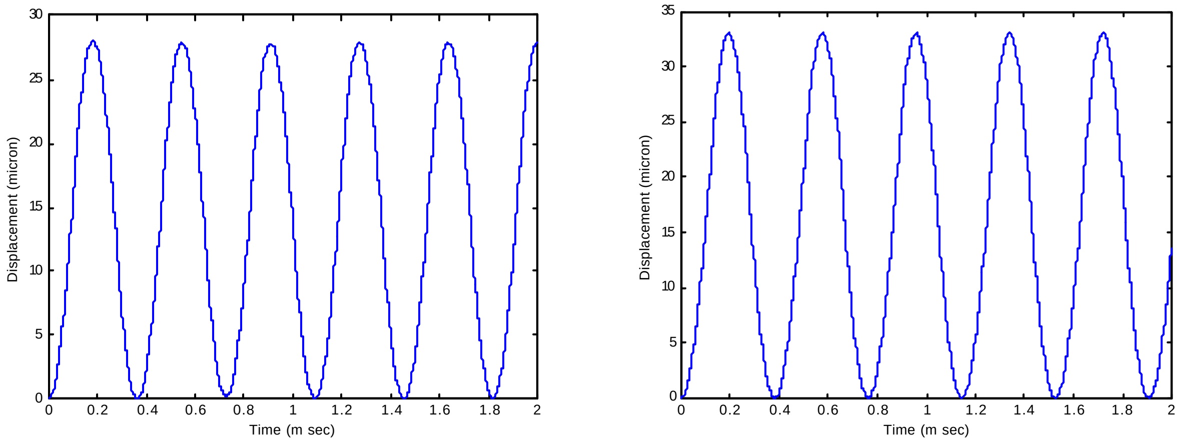

a b

Fig. (5) periodical operation.

a- V=51.1 volts, x_1 = 28µm,T_1=108.3µsec, T_2=181.3µsec, T_3=278.6µsec, T_2=363.6µsec, freq. = 2.75khz.

b- V=51.1 volts, x_1 = 33µm,T_1=131.8µsec, T_2=193.6µsec, T_3=282.8µsec, T_2=381.5µsec, freq. = 2.62khz.

Conclusion

We have reported a new digital compensation technique to improve the dynamic response of the comb-drive actuator. The improvement is achieved in reducing both the overshoot and the rise time in the actuator response. This enables to dynamically operate the actuator to nearly its maximum allowable displacement determined from the static analysis without having a sticking problem. In addition this technique has shown the capacity to move the actuator with a frequency response higher than its resonance frequency in a non-sustained operation mode.

References

[1] William C. Tang, Tu-Cuong H. Nguyen and Roger T. Howe, Laterally driven polysilicon resonant microstructures , IEEE Micro Electro Mechanical Systems Workshop, Salt Lake City, UT, U.S.A., pp. 53-59, Feb. 20-22, 1989.

[2] W. C. Tang, T. H. Nguyen, M. W. Judy, and R. Howe, Electrostatic-comb drive for lateral polysilicon resonators , Technical Digest, 5th International conference on Solid-State Sensors and Actuators, Montreux, Switherland, pp. 138-140, June 25-30, 1989.

[3] Chang-Jin Kim, Albert P. Pisano, Richard S. Muller and Martin G. Lim, Polysilicon Microgripper , Technical Digest IEEE Solid-State Sensors and Actuator Workshop, pp. 48-51, June, 1990.

[4] J. J. Sniegowski and E. J. Garci, Microfabricated actuators and their applications to optics , in Proceeding SPIE, vol. 2383, pp. 46-64, 1995.

[5] W. Ye, S. Mukherjee and N. C. McDonald, Optimal shape design of an electrostatic comb drive in micromechanical systems , Journal of Microelectromechnical Systems, vol. 7, No. 1, pp. 16-26, March 1998.

[6] W. A. Johnson and L. K. Warne, Electrophysics of micromechanical comb actuators , Journal of Microelectromechnical Systems, vol. 4, No. 1, pp. 49-59, March 1995.

[7] Cornel Marxer, Patrick Griss, and Nicolaas F. de Rooij, A variable optical attenuator based on silicon Micromechanics , IEEE Photonics Technology Letters, vol. 11, No. 2, February 1999.

[8] V. P. Jaecklin, C Linder and N. F. de Rooij and J M Moret, Micromechanical comb actuators with low driving voltage , J. Micromech. Microeng, pp. 250-255, 1992.

[9] Y. Chen, Y. Shroff, W. G. Oldham, Phase-lead Compensator to Improve the Transient Performance of Comb Actuator, Technical Proceedings of the Third International Conference on Modeling and Simulation of Microsystems, pp. 178-180, 2000.

[10] Y. Chen, Control and Shape Design of an Electrically-Damped Comb Drive for the Digital Operation, Proceedings of SPIE: MOEMS and Miniaturized Systems, Vol. 4178, pp. 387-394, Santa Clara, 2000.

[11] William T. Thomson, Theory of Vibrations with applications , Prentice-Hall Inc., Englewood Cliffs, New Jersy, pp. 95-98, 1972.